Front. Optoelectron. China 2011, 4(1): 80–86
DOI 10.1007/s12200-011-0209-y

RESEARCH ARTICLE

Effect of deoxycholic acid on performance of dye-sensitized solar cell based on black dye

Quanyou FENG, Hong WANG, Gang ZHOU, Zhong-Sheng WANG (✉)

Department of Chemistry, Laboratory of Advanced Materials, Fudan University, Shanghai 200438, China

Abstract The effect of coadsorption with deoxycholic acid (DCA) on the performance of dye-sensitized solar cell (DSSC) based on $[(C_4H_9)_4N]_3[Ru(Htcterpy)(NCS)_3]$ (tcterpy = 4,4′,4″-tricarboxy-2,2′:6′,2″-terpyridine), a so-called black dye, had been investigated. Results showed that the coadsorption of DCA with the black dye results in significant improvement in the photocurrent and mild increase in the photovoltage, which leads to an enhancement of overall power conversion efficiency by 9%. The enhancement of photocurrent was attributed to the increased efficiency of charge collection and/or electron injection. The coadsorption with DCA suppressed charge recombination and thus improved open-circuit photovoltage.

Keywords dye-sensitized solar cell (DSSC), coadsorption, black dye

1 Introduction

Due to the fast depletion of the reserves of fossil fuel and global warm as well as the problems of environmental pollution coming from the consumption of fossil fuel, there has been an intensive search for a renewable energy, which is cost-effective and clean energy [1]. Affluent solar energy has been widely considered as a major supply of sustainable energy. The performance/price ratio of photovoltaic devices will determinate whether they will be selected for solar energy in the end [2,3]. In this context, dye-sensitized solar cells (DSSCs) have been attracting remarkable attentions of researchers due to their productions with low cost, environmental friendliness and high conversion efficiency of solar-to-electric power [4].

A DSSC consisits of four major parts: a film of nanocrystalline semiconductor of metal oxide, dye sensitizer, redox electrolyte, and counter electrode. As a crucial part of DSSC, numerous dye sensitizers have been prepared for aims to decrease the cost of fabrication and improve the performance of DSSCs toward high conversion efficiency and good stability [5–16]. Up to now, more renowned Ru(II)-polypyridyl photosensitizers (such as N719 and black dye) among various dyes reported for the applications of DSSC, have shown the highest performance with power conversion efficiencie over 10% under air mass (AM) 1.5 sunlight [17–19].

To date, detailed studies on the performance of solar cell, spectroscopic measurements, electrolyte composition and the kinetics of electron transfer of DSSCs based on the black dye (Fig. 1) have been fully investigated [5,20,21]. However, the aggregation of the black dye formed on the surface of the nanocrystalline semiconductor always shortens the lifetime of excited electrons, which results in decreased photocurrent and reduced efficiency of power conversion. In this case, it is necessary to break up the aggregation of the black dye on titanium dioxide (TiO_2) surface. In our previous work [22], we found that deoxycholic acid (DCA) can be used as a coadsorbate to suppress the aggregation of the dye sensitizer and thus to improve short-circuit photocurrent (J_{sc}) and open-circuit photovoltage (V_{oc}). Herein, we studied the coadsorption effect of DCA on conduction band (CB) edge shift and the suppression of charge recombination in DSSCs by means of ultraviolet-visible (UV-vis) absorption spectroscopy, cyclic voltammetry (CV), dark current and electrochemical impedance spectroscopy.

2 Experiments

2.1 Materials and reagents

The black dye was purchased from Solaronix S. A., Aubonne, Switzerland and used as received. DCA, lithium iodide (LiI), I_2, 4-*tert*-butylpyridine (TBP) and acetonitrile

Received October 18, 2010; accepted December 30, 2010

E-mail: zs.wang@fudan.edu.cn

(AN) were obtained from Acros. The redox electrolyte contains 0.1 M LiI, 0.05 M iodine (I_2), 0.6 M 1,2-dimethyl-3-*n*-propylimidazolium iodide (DMPImI) (Sinopharm Chemical Reagent Co. Ltd., China), and 0.5 M TBP using dehydrated AN as solvent. Conducting glass (fluorine-doped SnO_2, 10 Ω/square) was received from Nippon Sheet Glass Co., Japan. All solvents and chemicals used in this study were of reagent grade.

2.2 Fabrications and evaluations of DSSCs

TiO_2 films were fabricated on a conducting glass using a screen printing method with a paste consisting of about 23 nm TiO_2 particles available from our previous study [23]. To minimize experimental error arising from the difference of film thickness, 6.50±0.05 μm films obtained in one batch were rigorously selected for the fabrication of DSSCs. Black dye solutions (0.2 mM) with or without 20 mM DCA were prepared in ethanol and used to sensitize TiO_2 electrodes by immersing the TiO_2 films in these dye solutions overnight when they were at about 100°C and then they cooled from the heating. These DSSCs were assembled and encapsulated with a previous method [19]. To avoid diffuse light penetrating into active dye-loaded film, a metal black mask with an aperture area of 0.2354 cm^2 was employed to test photovoltaic performance. The photovoltaic performance of the DSSCs was measured with a Keithley 2400 Source Meter (Oriel) under illumination of simulated AM1.5 G solar light coming from a solar simulator (Oriel-91193 equipped with a 1000 W Xe lamp and an AM 1.5 filter). Incident light intensity was calibrated with a standard Si solar cell (Newport 91150). Action spectra of incident monochromatic photon-to-electron conversion efficiency (IPCE) for the solar cells were obtained with an Oriel-74125 system (Oriel Instruments). The intensity of monochromatic light was measured with a Si detector (Oriel-71640).

2.3 Instrumentations

The UV-vis absorption spectra of black dye and black dye/DCA in ethanol solution and nanocrystalline TiO_2 films were recorded with a Shimadzu model 3100 UV-vis-NIR spectrophotometer in transmission mode. CV experiments were performed with an Autolab analyzer using a typical three-electrode single-compartment cell equipped with dye-adsorbed TiO_2 on conductive glass as a working electrode, a platinum (Pt) wire as a counter electrode, and an Ag/Ag^+ electrode as a reference electrode. These measurements were carried out in a solution of lithium perchlorate (0.1 M) in water-free AN at a scan rate of 50 $mV \cdot s^{-1}$ at room temperature under nitrogen. The potential of the reference electrode was calibrated by ferrocene, and all potentials mentioned in this work are against normal hydrogen electrode (NHE). Impedance spectra for DSSCs under dark were measured with an impedance/gain-phase analyzer (Solartron SI 1260) connected with a potentiostat (Solartron SI 1286). The spectra were scanned in a frequency range of 10^{-1}–10^5 Hz at room temperature. The applied bias and alternating current amplitude were set at open-circuit condition and 10 mV, respectively.

3 Results and discussion

3.1 UV-Vis absorption spectra

Figure 2 shows the UV-vis absorption spectra of black dye and black dye/DCA in ethanol solution (0.2 mM). The absorption spectrum of the black dye is dominated by metal-to-ligand charge-transfer transitions (MLCT) [5]. Two MLCT transition bands are observed at 417 and 618 nm, which is in good agreement with previous study [5,20,21]. The band at 329 nm with a distinct shoulder at 340 nm is assigned to the intraligand π-π* transition of the 4,4′,4″-tricarboxy-2,2′:6′,2″-terpyridine ligand [24]. It should be noted that, upon the addition of DCA, the MLCT transition bands at 417 and 618nm are bathochromically shifted to 421 and 620 nm, respectively. It can be attributed to the protonation of the black dye when DCA was added in dye solution, which led to lowered energy level for the π* orbital. The protonation is illustrated in Eq. (1), where R stands for black dye excluding the two *tert*-butyl ammonium carboxylates. Upon mixing of DCA with the black dye, cation exchange

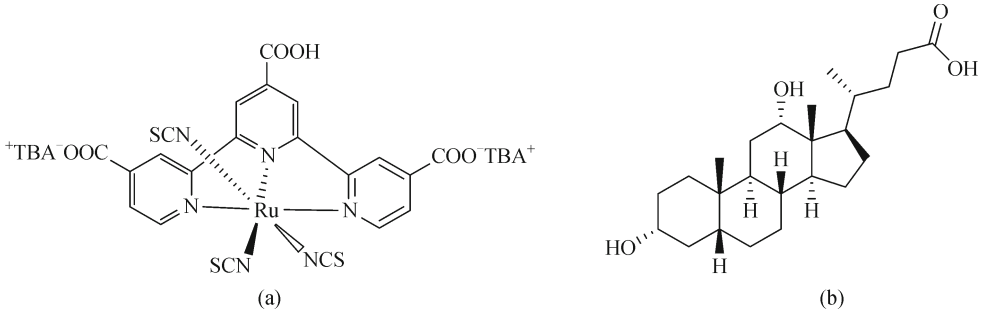

Fig. 1 Molecular structures of black dye (a) and DCA (b). TBA stands for tetrabutylammonium

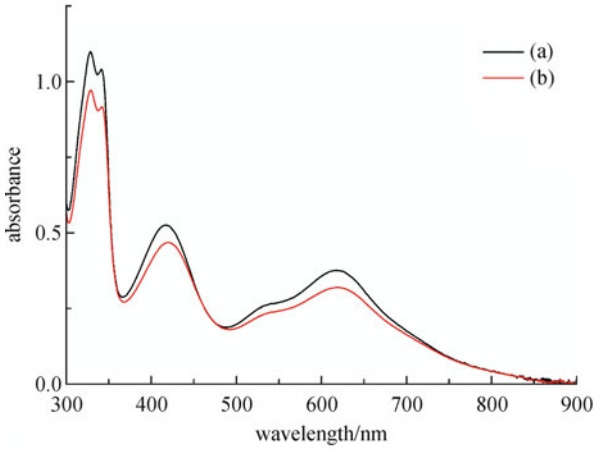

Fig. 2 UV-vis absorption spectra of the black dye in ethanol. (a) Without DCA; (b) with 20 mM DCA

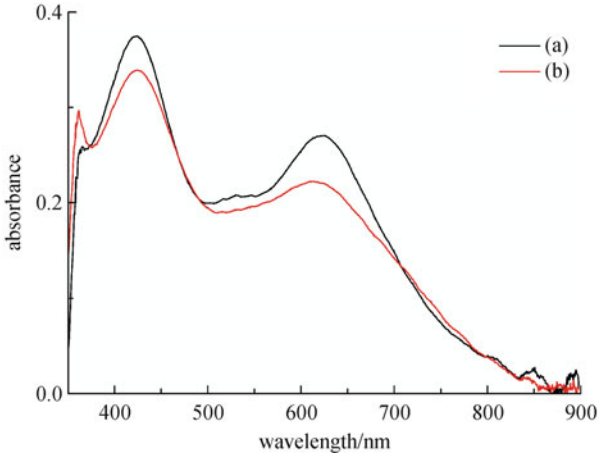

Fig. 3 UV-vis absorption spectra of TiO_2 films (1.8 μm) exposed to 0.2 mM black dye solution. (a) Without DCA; (b) with 20 mM DCA. The bare TiO_2 film (transparent) was used as a reference for the spectrum scan

occurs between the dye and DCA, and, as a consequence, more protons exist in the dye molecule. Nazeeruddin et al. reported that the MLCT transition bands of the black dye are bathochromically shifted by about 30 nm when the solution pH is lowered from 11 to 2 [5]. They concluded that the bathochromic shift was mainly due to the stronger electron-withdrawing ability of the protonated COOH groups compared to the carboxylic anions, which lowers the energy level of the π* orbital of the terpyridyl ligand.

$$\mathrm{R(COO^-TBA^+)_2} \overset{\mathrm{DCA}}{\rightleftharpoons} \mathrm{HOOCRCOO^-TBA^+} \overset{\mathrm{DCA}}{\rightleftharpoons} \mathrm{R(COOH)_2} \quad (1)$$

It is interesting to note that when 20 mM DCA is dissolved in black dye solution, the maximum UV-vis absorbance at the lowest energy MLCT peak decreased from 0.377 to 0.320 by 15%. This decrease stems from the presence of DCA, which probably affects the MLCT transition and thus decreases the molar extinction coefficient.

Figure 3 displays the UV-vis absorption spectra of the black dye on TiO_2 with and without DCA coadsorption. Compared with the spectrum of the black dye solution, a slight bathochromic shift from 618 to 624 nm is observed due to the interaction of the anchoring group with the titania surface, upon dye adsorption onto TiO_2 electrode. Similar red shift has been reported in several organic dyes on TiO_2 electrodes [25,26]. The degrees of dye adsorption on the TiO_2 electrodes are proportional to the intensity of the dye absorption. After 20 mM DCA is added in the dye immersing solution, the maximum absorbance at the lowest energy MLCT peaks decreases from 0.27 to 0.22. The dye amount on the TiO_2 surface reduces by 19%, which indicates that the dye and DCA compete for sites on the TiO_2 surface in an equilibrium process [22,27]. When 20 mM DCA is dissolved in the dye solution, the absorption spectra of the black dye is bathochromically shifted. However, as shown in Fig. 3, the peak position, which is the same as the dye/DCA solution case, does not shift upon coadsorption of DCA onto TiO_2 surface. This is because proton and Ti^{4+} have similar electron-withdrawing ability.

3.2 Electrochemical properties

The electrochemical properties of the black dye and black dye/DCA adsorbed onto TiO_2 film (6 μm) were investigated in 0.1 M lithium perchlorate ($LiClO_4$) (AN as the solvent) with N_2 bubble to degas the supporting electrolyte by CV.

Figure 4 shows the CV curves for dye-loaded TiO_2 films before and after coadsorption of DCA. The black dye displayed one reversible one-electron anodic oxidation step at half-wave potentials of 0.87 V versus NHE (same below). Similarly, the cografted TiO_2 electrode also exhibits one reversible couple at 0.87 V. The oxidation potential at 0.87 V is taken as the highest occupied molecular orbital (HOMO) energy level. Then the lowest unoccupied molecular orbital (LUMO) energy level is determined to be −0.56 V by

$$\mathrm{LUMO} = \mathrm{HOMO} - \mathrm{gap}, \quad (2)$$

where gap (1.43 eV) is the difference between the HOMO and LUMO levels and derived from the absorption threshold (870 nm) of dye-loaded TiO_2 film shown in Fig. 3. We therefore conclude that coadsorption of DCA with dye molecules has no obvious influence on both HOMO and LUMO levels.

Upon coadsorption, the CV signal decreased significantly and the current intensity decreases by 42% (Fig. 4), which is much larger than the drop in absorbance of 19% (Fig. 3). Such an interesting phenomenon has been

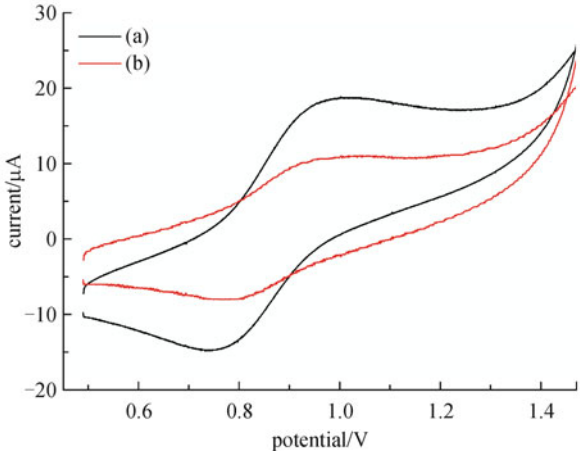

Fig. 4 Cyclic voltammograms of TiO_2 films after dipping in the following solutions. (a) 0.2 mM black dye; (b) 0.2 mM black dye + 20 mM DCA

reported in our previous study [22]. After the coadsorption of DCA, the significant decrease in current intensity in the CV curve suggests that DCA effectively suppresses the intermolecular interaction of dye molecules and weakens the electron hopping between two neighboring molecules. Therefore, DCA is favorable for suppressing the recombination of electrons with acceptors in a DSSC device.

3.3 Solar cell performance

Figure 5 compares the photocurrent action spectra before and after coadsorption with DCA, where the incident photon to current conversion efficiency (IPCE) is plotted as a function of wavelength. The IPCE values for DSSC based on black dye/DCA are much higher than those for black dye without DCA in the whole visible region. The maximum IPCE value increases from 68% to 75% by 10%. As IPCE is a product of light-harvesting efficiency (LHE), the electron injection efficiency (Φ_{inj}), and charge collection efficiency (Φ_c), as illustrated in Eq. (3), it is interesting to analyze which factor affects IPCE. Since LHE approaches 100% with 25 μm film based on the absorbance shown in Fig. 3, LHE should be reduced slightly upon DCA coadsorption. Therefore, the IPCE improvement is attributed to the enhancements of the electron injection yield and/or the charge collection yield, which will be discussed later.

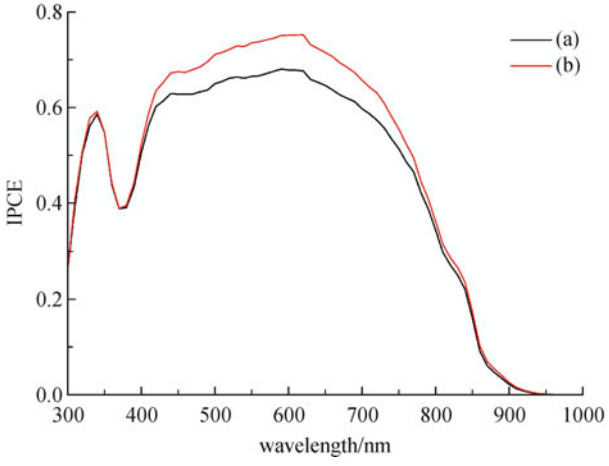

Fig. 5 IPCE action spectra of DSSCs based on (a) black dye; (b) black dye/DCA with scattering films (25 μm)

$$\mathrm{IPCE}(\lambda) = \mathrm{LHE}(\lambda) \times \Phi_{inj} \times \Phi_c. \quad (3)$$

The performance of DSSCs with and without DCA as a coadsorbate was tested. The current density – voltage (*J-V*) curves are shown in Fig. 6 and the corresponding data are summarized in Table 1. Upon coadsorption of DCA, the J_{sc} and V_{oc} increase while fill factor (*FF*) remains almost unchanged, resulting in an increase in overall efficiency (η) by 9% from 8.91% to 9.74%. Moreover, it is worthy to note the remarkably enhanced J_{sc} (by 1.14 mA/cm^2) and slight improvement in V_{oc} (20 mV) after coadsorption with DCA. According to our previous study [28], upon coadsorption with DCA, the TiO_2 surface is protonated and the CB shifts positively due to the proton adsorption. This positive shift of CB enlarges driving force for electron injection, which results in the enhanced IPCE and J_{sc}. In addition, coadsorption can break up dye aggregation, and the non-aggregated dye molecules are favorable for electron injection.

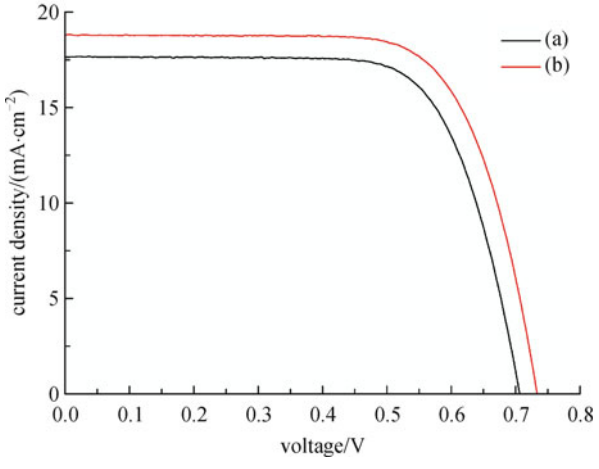

Fig. 6 *J-V* curves for DSSCs incorporating (a) black dye; (b) black dye /DCA with scattering films (25 μm)

Table 1 Effect of coadsorption of DCA on the photovoltaic performance of the DSSC

	J_{sc}/(mA·cm^{-2})	V_{oc}/V	*FF*	η/%
black dye	17.67	0.71	0.71	8.91
black dye/DCA	18.81	0.73	0.71	9.74

Since V_{oc} is theoretically the difference between the Fermi energy level of TiO_2 under light and the redox potential of the redox couple I_3^-/I^-, the positive shift of conduction band edge upon adsorption with DCA will result in a decrease in V_{oc}. However, V_{oc} increases mildly by 20 mV after coadsorption with DCA in this study, as listed in Table 1. This enhancement of V_{oc} can be attributed to the suppression of charge recombination between the injected electrons and I_3^- ions on the TiO_2 surface by DCA coadsorption, which was analyzed by dark current and electrochemical impedance spectroscopy.

3.4 Charge recombination

Coadsorption of DCA is expected to inhibit dye aggregation and hence retard charge recombination. Although the dark current is not a direct measurement of the charge recombination process under illumination, it is usually employed to compare the recombination rate under different conditions [29,30]. The *J-V* curves (Fig. 7) obtained from the solar cells based on black dye and black dye/DCA without light (dark current) indicate that the black dye has a more negative onset potential for the reduction of I_3^- upon coadsorption with DCA, which suggests that the coadsorption of DCA reduces the electron recombination between injected electrons the TiO_2 surface and I_3^-.

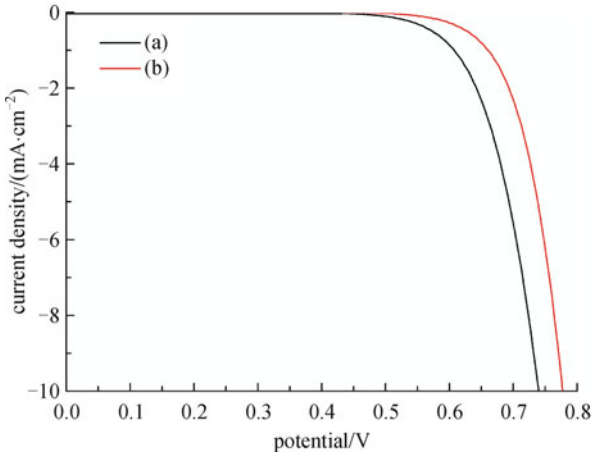

Fig. 7 Dark current with applied potential for DSSCs based on (a) black dye; (b) black dye/DCA

To further understand the V_{oc} enhancement upon coadsorption with DCA, electrochemical impedance spectra were recorded in dark and shown in Fig. 8. The semicircle in the intermediate frequency regime represents the electron transfer at the TiO_2/dye/electrolyte interface [31]. A larger radius of the semicircle in this intermediate frequency regime implies a lower rate of charge recombination between injected electrons and electron acceptors in the redox electrolyte. In dark at a forward bias of 0.71 V,

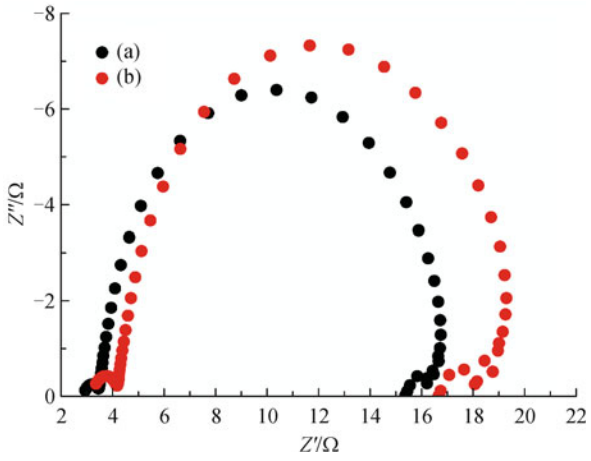

Fig. 8 Electrochemical impedance spectra of DSSCs based on (a) black dye; (b) black dye/DCA

the radius of this semicircle increases to some extent upon coadsorption with DCA as shown in Fig. 8, indicating effective suppression of the back reaction of the injected electron with I_3^- ions. As demonstrated in our previous work [22], this retardation of charge recombination can bring about a voltage gain, which compensates for the voltage loss arising from the CB shift due to DCA coadsorption. As a consequence, a moderate improvement in V_{oc} is observed upon coadsorption of DCA.

4 Conclusions

The effect of coadsorption of the DCA on the photovoltaic performance of the DSSC based on the black dye was studied. We found that DCA could improve photocurrent by 6% and photovoltage by 20 mV. As a consequence, overall efficiency enhancement by 9% was realized upon DCA coadsorption.

Acknowledgements This work was financially supported by the National Natural Science Foundation of China (Grant Nos. 20971025, 90922004, and 50903020), the Shanghai Pujiang Project (No. 09PJ1401300), and the Shanghai Non-Governmental International Cooperation Program (No. 10530705300), National Basic Research Program of China (No. 2011CB933302), Shanghai Leading Academic Discipline Project (No. B108), the Project sponsored by SRF for ROCS, SEM, and Jiangsu Major Program (No. BY2010147).

References

1. Robertson N. Optimizing dyes for dye-sensitized solar cells. Angewandte Chemie International Edition, 2006, 45(15): 2338–2345
2. Lewis N S. Toward cost-effective solar energy use. Science, 2007, 315(5813): 798–801

3. Xu M F, Wenger S, Bala H, Shi D, Li R Z, Zhou Y Z, Zakeeruddin S M, Grätzel M, Wang P. Tuning the energy level of organic sensitizers for high-performance dye-sensitized solar cells. Journal of Physical Chemistry C, 2009, 113(7): 2966–2973
4. O'Regan B, Grätzel M. A low cost, high efficiency solar cell based on dye-sensitized colloidal TiO_2 films. Nature, 1991, 353(6346): 737–740
5. Nazeeruddin M K, Péchy P, Renouard T, Zakeeruddin S M, Humphry-Baker R, Comte P, Liska P, Cevey L, Costa E, Shklover V, Spiccia L, Deacon G B, Bignozzi C A, Grätzel M. Engineering of efficient panchromatic sensitizers for nanocrystalline TiO_2-based solar cells. Journal of the American Chemical Society, 2001, 123(8): 1613–1624
6. Hara K, Kurashige M, Dan-oh Y, Kasada C, Shinpo A, Suga S, Sayama K, Arakawa H. Design of new coumarin dyes having thiophene moieties for highly efficient organic dye-sensitized solar cells. New Journal of Chemistry, 2003, 27(5): 783–785
7. Horiuchi T, Miura H, Sumioka K, Uchida S. High efficiency of dye-sensitized solar cells based on metal-free indoline dyes. Journal of the American Chemical Society, 2004, 126(39): 12218–12219
8. Hagberg D P, Edvinsson T, Marinado T, Boschloo G, Hagfeldt A, Sun L C. A novel organic chromophore for dye-sensitized nanostructured solar cells. Chemical Communications, 2006, 21 (21): 2245–2247
9. Choi H, Baik C, Kang S O, Ko J, Kang M S, Nazeeruddin M K, Grätzel M. Highly efficient and thermally stable organic sensitizers for solvent-free dye-sensitized solar cells. Angewandte Chemie International Edition, 2008, 47(2): 327–330
10. Nazeeruddin M K, Kay A, Rodicio I, Humphry-Baker R, Muller E, Liska P, Vlachopoulos N, Grätzel M. Conversion of light to electricity by Cis-X2bis(2,2'-Bipyridyl-4,4'-Dicarboxylate)Ruthenium(II) charge-transfer sensitizers (X = Cl^-, Br^-, I^-, CN^-, and SCN^-) on nanocrystalline TiO_2 electrodes. Journal of the American Chemical Society, 1993, 115(14): 6382–6390
11. Wang Z-S, Koumura N, Cui Y, Takahashi M, Sekiguchi H, Mori A, Kubo T, Furube A, Hara K. Hexylthiophene-functionalized carbazole dyes for efficient molecular photovoltaics: tuning of solar cell performance by structural modification. Chemistry of Materials, 2008, 20(12): 3993–4003
12. Ning Z, Zhang Q, Wu W, Pei H, Liu B, Tian H. Starburst triarylamine based dyes for efficient dye-sensitized solar cells. Journal of Organic Chemistry, 2008, 73(10): 3791–3797
13. Islam A, Sugihara H, Yanagida M, Hara K, Fujihashi G, Tachibana Y, Katoh R, Murata S, Arakawa H. Efficient panchromatic sensitization of nanocrystalline TiO_2 films by beta-diketonato ruthenium polypyridyl complexes. New Journal of Chemistry, 2002, 26(8): 966–968
14. Wang P, Humphry-Baker R, Moser J E, Zakeeruddin S M, Grätzel M. Amphiphilic polypyridyl ruthenium complexes with substituted 2,2'-dipyridylamine ligands for nanocrystalline dye-sensitized solar cells. Chemistry of Materials, 2004, 16(17): 3246–3251
15. Altobello S, Argazzi R, Caramori S, Contado C, Da Fré S, Rubino P, Choné C, Larramona G, Bignozzi C A. Sensitization of nanocrystalline TiO_2 with black absorbers based on Os and Ru polypyridine complexes. Journal of the American Chemical Society, 2005, 127 (44): 15342–15343
16. Kitamura T, Ikeda M, Shigaki K, Inoue T, Anderson N A, Ai X, Lian T, Yanagida S. Phenyl-conjugated oligoene sensitizers for TiO_2 solar cells. Chemistry of Materials, 2004, 16(9): 1806–1812
17. Grätzel M. Conversion of sunlight to electric power by nanocrystalline dye-sensitized solar cells. Journal of Photochemistry and Photobiology A Chemistry, 2004, 164(1–3): 3–14
18. Nazeeruddin M K, De Angelis F, Fantacci S, Selloni A, Viscardi G, Liska P, Ito S, Takeru B, Grätzel M G. Combined experimental and DFT-TDDFT computational study of photoelectrochemical cell ruthenium sensitizers. Journal of the American Chemical Society, 2005, 127(48): 16835–16847
19. Wang Z-S, Yamaguchi T, Sugihara H, Arakawa H. Significant efficiency improvement of the black dye-sensitized solar cell through protonation of TiO_2 films. Langmuir, 2005, 21(10): 4272–4276
20. Bauer C, Boschloo G, Mukhtar E, Hagfeldt A. Interfacial electron-transfer dynamics in Ru(tcterpy)(NCS)3-sensitized TiO_2 nanocrystalline solar cells. Journal of Physical Chemistry B, 2002, 106(49): 12693–12704
21. Hara K, Nishikawa T, Kurashige M, Kawauchi H, Kashima T, Sayama K, Aika K, Arakawa H. Influence of electrolyte on the photovoltaic performance of a dye-sensitized TiO_2 solar cell based on a Ru(II) terpyridyl complex photosensitizer. Solar Energy Materials and Solar Cells, 2005, 85(1): 21–30
22. Ren X M, Feng Q Y, Zhou G, Huang C H, Wang Z-S. Effect of cations in coadsorbate on charge recombination and conduction band edge movement in dye-sensitized solar cells. Journal of Physical Chemistry C, 2010, 114(15): 7190–7195
23. Wang Z-S, Kawauchi H, Kashima T, Arakawa H. Significant influence of TiO_2 photoelectrode morphology on the energy conversion efficiency of N719 dye-sensitized solar cell. Coordination Chemistry Reviews, 2004, 248(13–14): 1381–1389
24. Nazeeruddin M K, Pechy P, Grätzel M. Efficient panchromatic sensitization of nanocrystalline TiO_2 films by a black dye based on a trithiocyanato-ruthenium complex. Chemical Communications, 1997, 18(18): 1705–1706
25. Sayama K, Tsukagoshi S, Hara K, Ohga Y, Shinpou A, Abe Y, Suga S, Arakawa H. Photoelectrochemical properties of J aggregates of benzothiazole merocyanine dyes on a nanostructured TiO_2 film. Journal of Physical Chemistry B, 2002, 106(6): 1363–1371
26. Sayama K, Hara K, Mori N, Satsuki M, Suga S, Tsukagoshi S, Abe Y, Sugihara H, Arakawa H. Photosensitization of a porous TiO_2 electrode with merocyanine dyes containing a carboxyl group and a long alkyl chain. Chemical Communications, 2000, 13(13): 1173–1174
27. Neale N R, Kopidakis N, van de Lagemaat J, Grätzel M, Frank A J. Effect of a coadsorbent on the performance of dye-sensitized TiO_2 solar cells: shielding versus band-edge movement. Journal of Physical Chemistry B, 2005, 109(49): 23183–23189
28. Wang Z-S, Zhou G. Effect of surface protonation of TiO_2 on charge recombination and conduction band edge movement in dye-sensitized solar cells. Journal of Physical Chemistry C, 2009, 113 (34): 15417–15421
29. Gregg B A, Pichot F, Ferrere S, Fields C L. Interfacial

recombination processes in dye-sensitized solar cells and methods to passivate the interfaces. Journal of Physical Chemistry B, 2001, 105(7): 1422–1429

30. Choi H, Raabe I, Kim D, Teocoli F, Kim C, Song K, Yum J H, Ko J, Nazeeruddin M K, Grätzel M. High molar extinction coefficient organic sensitizers for efficient dye-sensitized solar cells. Chemistry-a European Journal, 2010, 16(4): 1193–1201
31. Wang Q, Moser J E, Grätzel M. Electrochemical impedance spectroscopic analysis of dye-sensitized solar cells. Journal of Physical Chemistry B, 2005, 109(31): 14945–14953